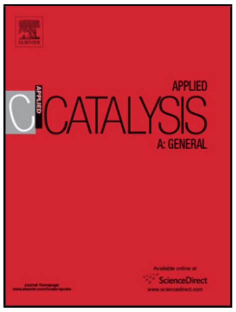

# $CO_2$ Fixation by Cycloaddition of Mono/Disubstituted Epoxides using Acyl Amide Decorated Co(II) MOF as a Synergistic Heterogeneous Catalyst

Parth Patel, Bhavesh Parmar, Renjith S. Pillai, Amamudin Ansari,
Noor-ul H. Khan, Eringathodi Suresh

PII: S0926-860X(19)30530-7
DOI: https://doi.org/10.1016/j.apcata.2019.117375
Reference: APCATA 117375

To appear in: *Applied Catalysis A, General*

Received Date: 11 October 2019
Revised Date: 3 December 2019
Accepted Date: 6 December 2019

Please cite this article as: Patel P, Parmar B, Pillai RS, Ansari A, Khan N-ulH, Suresh E, $CO_2$ Fixation by Cycloaddition of Mono/Disubstituted Epoxides using Acyl Amide Decorated Co(II) MOF as a Synergistic Heterogeneous Catalyst, *Applied Catalysis A, General* (2019), doi: https://doi.org/10.1016/j.apcata.2019.117375

# $CO_2$ Fixation by Cycloaddition of Mono/Disubstituted Epoxides using Acyl Amide Decorated Co(II) MOF as a Synergistic Heterogeneous Catalyst

**Parth Patel [a][c]† , Bhavesh Parmar [b][d]† , Renjith S. Pillai [e] , Amamudin Ansari [a][d] ,Noor-ul H. Khan*[a][c][d] nhkhan@csmcri.res.in and Eringathodi Suresh*[b][d] esuresh@csmcri.res.in; sureshe123@rediffmail.com**

[a] Inorganic Materials and Catalysis Division, CSIR-Central Salt and Marine Chemicals Research Institute, G. B. Marg, Bhavnagar 364 002, Gujarat, India.
[b] Analytical and Environmental Science Division and Centralized Instrument Facility, CSIR-Central Salt and Marine Chemicals Research Institute, G. B. Marg, Bhavnagar 364 002, Gujarat, India.
[c] Charotar University of Science & Technology, Changa-388 421, Anand, Gujarat, India.
[d] Academy of Scientific and Innovative Research (AcSIR), Ghaziabad - 201 002, India.
[e] Department of Chemistry, Faculty of Engineering and Technology, SRM Institute of Science and Technology, Kattankulathur - 603 203, Chennai, India.
† These authors contributed equally.

**Graphical abstract**

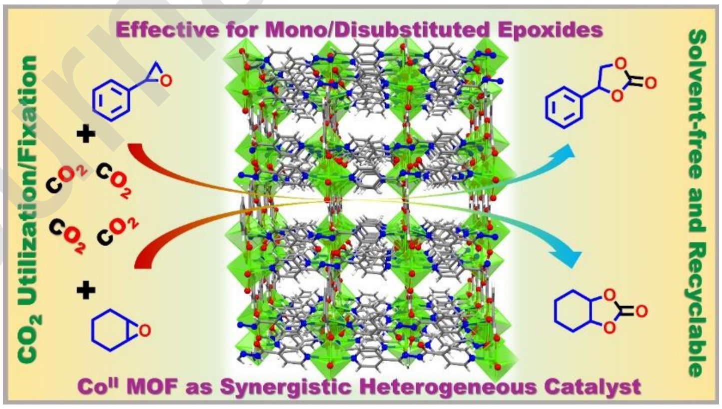

**Graphical Abstract Text**

Co(II) MOF as an efficient heterogeneous catalyst for conversion of $CO_2$ and mono/disubstituted epoxide to value added cyclic carbonate product at mild reaction conditions has been reported.

## Highlights

- Dual ligand 3D MOF {[Co(**BDC**)(**L**)]·$2H_2O$.xG}$_n$ (**CoMOF-2**) was synthesized via a simple room temperature stirring method.
- Bulk Phase purity of **CoMOF-2** was assessed by various physicochemical method, including Powder X- ray diffraction (PXRD).
- **CoMOF-2** act as an efficient binary heterogeneous catalyst for $CO_2$ sequestration with mono/disubstituted epoxides at moderate reaction condition to value added organic carbonate with excellent yield and recyclability.
- $CO_2$ adsorption by **CoMOF-2**, Lewis acidic metal and the basic –NH on N-donor linker enable the interactions and activation of epoxide with $CO_2$ molecules towards excellent performance in the chemical fixation of $CO_2$.

**Abstract:** Dual ligand 3D MOF {[Co(**BDC**)(**L**)]·$2H_2O$.xG}$_n$ (**CoMOF-2**; G = guest) was synthesized via simple room temperature stirring method. Bulk Phase purity of **CoMOF-2** was assessed by various physicochemical methods including X- ray diffraction (XRD). $CO_2$ adsorption isotherms indicate that activated **CoMOF-2** is efficient in $CO_2$ uptake, which has been utilized for the $CO_2$-Epoxide cycloaddition. The catalytic ability of **CoMOF-2** as a binary catalyst revealed excellent results for variety of monosubstituted epoxide under solvent- free conditions (1 bar/40 °C/12 h). Interestingly **CoMOF-2/**KI also showed great potential as a heterogeneous catalyst for disubstituted epoxide (10 bar/120 °C/24 h) with high yields/selectivity. The catalytic efficiency of the present investigation for scantly explored disubstituted epoxide is better/on par with the earlier reports and the recyclability of the catalyst is an added advantage. Probable mechanism for the catalytic reaction is deduced and verified the representative energy profile for cycloaddition of $CO_2$-Cyclohexane oxide (CHO) by DFT calculation.

**Keywords:** Metal-Organic Frameworks / $CO_2$ Capture & Conversion / Heterogeneous Catalysis / Disubstituted Epoxides / Cyclic Carbonate / DFT calculation.

## Introduction

Great progress in catalysis has been made in recent years in $CO_2$ mitigation via sustainable conversion of $CO_2$ into value added chemicals. Very recently, $CO_2$ capture and utilization have attracted tremendous research interest owing to green and sustainable concerns.[1-6] Important chemical reactions and transformation such as oxidation of alcohols, amines, sulfides and utilization of $CO_2$ in cycloaddition reactions etc. have been achieved by newly developed material as catalytic system, particularly coordination complexes to realize these organics transformation.[7-12] However, coordination complexes generally act as a homogenous catalyst and lacks limitations as an efficient catalyst due to separation and reusability issues, harsh reaction conditions product yield.[13-15] Thus, it is mandatory to develop efficient catalytic materials with green and selective transformation of organic chemicals. Carbon dioxide ($CO_2$) emitted from industries and burning of fossil fuel is not only considered as a greenhouse gas which has adverse effect on environment and global climate change, but has gained significant attention as a source of C1 building block for the synthesis of value-added chemicals.[1-6] Research efforts in this direction are in progress for the development of new materials for selective carbon dioxide capture and its subsequent utilization towards fine chemical synthesis. Therefore, it is a challenge for researchers and significant attention has been paid for the development competent catalytic systems for efficient $CO_2$ capture and its utilization at ambient condition.[1-6] In this context, sustainable $CO_2$ sequestration to produce cyclic carbonates with good high yield and selectivity has been considered as an atom economic process by cycloaddition reaction with epoxide.[11-12,16-19] However, kinetic inertness and the thermodynamic stability of $CO_2$ are major concern for its conversion at ambient conditions and to achieve this task development of ideal heterogeneous catalyst with good chemical stability and recyclability is anticipated. Interestingly, cyclic carbonates are value added chemical intermediates and find extensive applications in the production of pharmaceuticals, fine chemicals and as an electrolyte in Li-ion battery.[20-27]

Metal−organic frameworks (MOFs) constructed from functionally decorated organic linkers coupled with metal ions/clusters generating aesthetic multidimensional network are promising materials owing to their tunable structure-property features aimed at various applications including catalysis.[28-37] For accomplishing $CO_2$ emission mitigation targets, one of the requisite protocols for $CO_2$ capture and utilization is development of chemically stable porous materials as a heterogeneous catalyst with high $CO_2$ uptake in cycloaddition with variety of epoxides to industrially important molecules.[38-42] MOFs are the suitable candidate for this purpose and the most significant feature is their porosity, and both metal center as well as functionally decorated tailor-made organic linkers that can either access or activate the substrate and contribute towards the catalytic activity. Creating unsaturated open metal sites and integrating functional groups in ligands were adopted to increase $CO_2$ capture which in turn can favor performance of MOFs towards the synthesis of fine chemicals by sustainable approach in cycloaddition reaction.[41-44] Although , some of the celebrated MOFs for example MMPF-9, HKUST-1, MMFC-2, so on and some of our reports exhibited efficient catalytic activity under mild reaction condition in $CO_2$-epoxide cycloaddition.[45-79]

MOF based cycloaddition of $CO_2$ with disubstituted epoxide is not prevalent may be because of the harsh conditions to expedite. Hence, design and development of novel MOF as a heterogeneous catalyst with good chemical stability, with good $CO_2$ adsorption and conversion are the requirement to realize efficient catalysis under mild conditions including mono/disubstituted epoxides to value added cyclic carbonate, which has significance in energy conservation and environmental protection.

In this contribution, synthesis of Co (II) based mixed-ligand 3D MOF $\{[Co(\mathbf{BDC})(\mathbf{L})]\cdot 2H_2O.xG\}_n$ (**CoMOF-2**; G = guest) involving Benzene-1,4-dicarboxylic acid ($H_2$**BDC**) and N-donor Schiff base ligand **L** (4-pyridyl carboxaldehyde isonicotinoylhydrazone) by adaptable routes (room temperature stirring and diffusion method), and enlightened its utility as a heterogeneous catalyst for $CO_2$ sequestration as a heterogeneous catalyst. Crystals suitable for Single crystal x-ray diffraction (SXRD) analysis and bulk synthesis of the catalytic material has been realized by diffusion and room temperature (RT) stirring method respectively from the ligand precursors with Co(II) salt in appropriate stoichiometry. Structural analysis of **CoMOF-2** revealed 3D network and phase pure bulk material established by d analytical methods have been further utilized for the catalytic experiment. Remarkably, **CoMOF-2** has been identified as good heterogeneous catalysts for the cycloaddition of both mono and disubstituted epoxides with $CO_2$ to the respective cyclic carbonates yielding high conversion and selectivity. **CoMOF-2** showed excellent $CO_2$ conversion under ambient conditions with monosubstituted epoxide (solvent free, $P_{CO2}$ =1 bar, 40 $^{o}$C, 12 h), nevertheless catalytic reaction of disubstituted epoxides with good yield and selectively was achieved with harsh conditions as expected (solvent free, $P_{CO2}$ = 10 bar, 120 $^{o}$C, 24 h), but much superior than the scantly explored previous reports. The recycling performance of **CoMOF-2** revealed the catalyst was stable with only marginal loss of catalytic activity.

## Results and Discussion

### *Crystal Structure and Characterization of CoMOF-2*

SXRD analysis exposed **CoMOF-2** crystallized in the monoclinic space group C2/c, and the 3D framework is composed of dimeric Co(II)-carboxylate clusters generating a two dimensional $[M_2(\mathbf{BDC})_2]_n$ 2D *sql* sheets (**Figure 1a)** pillared by the N-donor ligand **L.** Three different **BDC** ligands are involved in coordination with each Co(II) metal center of the dimeric cluster and the symmetrically disposed **BDC** ligands are making $\mu_3$-$\eta^1\eta^1\eta^1\eta^1$ chelated bridging mode of coordination generating 2D $\{Co_2(\mathbf{BDC})_2\}_n$ sheets with Co(II)···Co(II) distance 4.11Å within the dimeric unit. Axial coordination by the terminal nitrogen from **L** across the 2D $\{Co_2(\mathbf{BDC})_2\}_n$ sheets with offset orientation along *bc*-plane generates an interpenetrated 3D framework (**Figure 1b**). As depicted in **figure 1c**, the located water molecules in **CoMOF-2** are encapsulated in the cavity down *b*-axis and are involved in strong O-H···O hydrogen bonding in bridging the interpenetrated 3D framework.

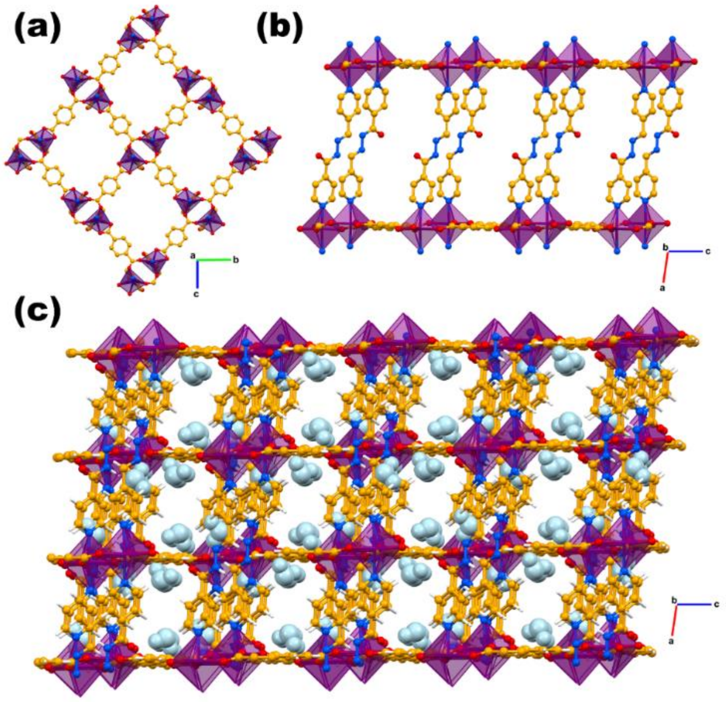

**Figure 1.** (a) Co(II)-carboxylate clusters generating $[M_2(\mathbf{BDC})_2]_n$ 2D sql sheets, (b) 2D $\{Co_2(\mathbf{BDC})_2\}_n$ sheets doubly pillared via axial coordination by **L**; (c) 3D interpenetrated framework with encapsulated water molecules in **CoMOF-2** viewed down b-axis.

MOFs with porosity and functionally decorated ligands, particularly amine/ acyl functional groups are known for their ability for the $CO_2$ capture.[80-84] Efficient $CO_2$ capture and manifestation of active sites in MOFs can favor catalytic conversion of $CO_2$ in cycloaddition of epoxide to value added chemicals. We reported harvesting crystals/bulk synthesis of **CoMOF-2** via different routes by diffusion method/room temperature stirring with good phase purity elsewhere.[85] The details pertaining to MOF synthesis and characterization are provided in the ESI (using powder X-ray diffraction (PXRD), FTIR and TGA). A brief account of product characterization and **CoMOF-2** crystal structure, purity, chemical/thermal stability of the pristine recovered catalyst after 6 cycles were characterized by different analytical methods. The simulated SXRD data of **CoMOF-2** is in full agreement with the experimental PXRD pattern of the MOFs synthesized via RT stirring as well as the recovered catalyst after 6 cycles establishing the phase purity/chemical stability of the catalyst (**Figure S1**).

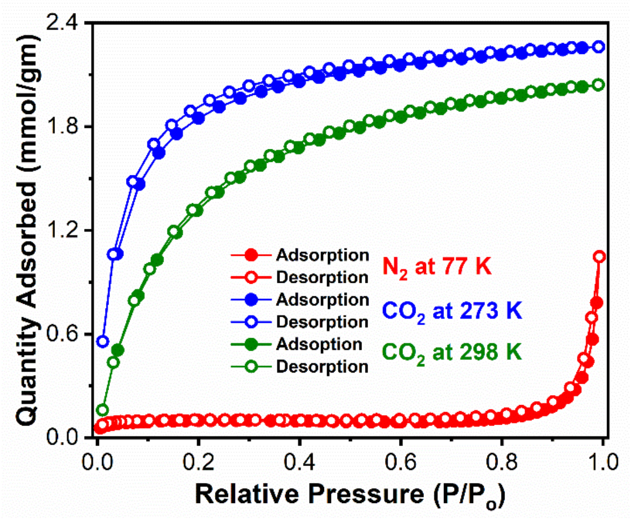

**Figure 2.** Comparisons of $N_2$ adsorption isotherm at 77 K and $CO_2$ adsorption isotherm measured at 273 K and 298 K for **CoMOF-2′**.

Good agreement of the FTIR data of pristine and recovered catalyst also support the structural integrity (**Figure S2**). TGA analysis of **CoMOF-2** disclosed good thermal stability up to ~330°C (**Figure S3**). FE-SEM images of the recovered catalyst after 6 cycles retained almost the same textural features of pristine catalyst (**Figure S4**). Gas sorption analysis of activated **CoMOF-2** exposed no significant $N_2$ uptake with BET surface area only 6.8 $m^2g^{-1}$. Pore size distribution measured at lower $P/P_0$ values revealed pore size in the range 6.89 Å and the average pore diameter was 24 Å (**Figure S5**). Adsorption analysis of $CO_2$ revealed promising results 51 $cm^3/g$ (2.26 mmol/g) and 45 $cm^3/g$ (2.04 mmol/g) respectively at 273K and 298K at 1 atm pressure (**Figure 2**). Interaction of the amide functional group of the pillared **L** in the framework favor the capture of polar $CO_2$, which is reinforced with calculated Isosteric heat ($Q_{st}$) for $CO_2$ adsorption using Clausius−Clapeyron equation (35.0 kJ $mol^{-1}$) from their experimental results (**Figure S6**). Adsorption of the polar $CO_2$ molecule inside the pore is established by GCMC calculation in our earlier report by interaction of carbonyl-group of **L** (with a mean characteristic $O(CO_2)$-$O_{Carbonyl}$ distances in the range of 2.8-3.5Å ) which also favors the catalytic performance by **CoMOF-2** in $CO_2$ utilization. (**Figure S7**)

### *Catalytic Cycloaddition of $CO_2$ with mono/disubstituted Epoxides*

**CoMOF-2** with Lewis acidic Co(II) center with weakly chelated carboxylate arm, presence of amide decorated Lewis basic site on **L** and $CO_2$ adsorption capacity encouraged us to investigate the catalytic activity for cycloaddition of both mono and disubstituted epoxides with $CO_2$. The optimization of reaction conditions revealed the requirement of TBAB /KI as a co-catalyst along with MOF catalyst for the high yield synthesis of cyclic carbonates. Styrene oxide (SO) and cyclohexane oxide (CHO) has been engaged as representative model substrates for mono/ disubstituted epoxide respectively for optimization of reaction conditions. The extracted catalytic products were identified by using GC and further analyzed by $^1H$ and $^{13}C$ NMR spectroscopy (**Figure S10-S29**). In catalytic reaction for monosubstituted epoxide, styrene oxide (SO) as a model substrate with 8.7 mmol, MOF/co-catalyst concentration (1.8 / 2.5 mol%) and 1 bar of $CO_2$ pressure has been kept fixed. Details of solvent free cycloaddition of $CO_2$ with SO tested for optimization conditions are given in **Table 1**.

**Table 1.** Cycloaddition of Styrene oxide (**SO**) and $CO_2$ for Styrene carbonate (**SC**) formation.*

| Entry | Catalyst/Co-catalyst | Temp. (ºC) | Time (h) | SO Con. (%)# |
|---|---|---|---|---|
| 1 | None | RT | 12 | 01 |
| 2 | TBAB | RT | 12 | 08 |
| 3 | **CoMOF-2** | RT | 12 | 09 |
| 4 | **CoMOF-2**/TBAB | RT | 12 | 51 |
| 5 | **CoMOF-2**/TBAI | RT | 12 | 34 |
| 6 | **CoMOF-2**/KI | RT | 12 | 48 |
| 7 | **CoMOF-2**/TBAB | 40 | 8 | 93 |
| 8 | **CoMOF-2**/TBAB | 40 | 12 | 99 |
| 9 | None | 40 | 12 | 03 |
| 10 | TBAB | 40 | 12 | 22 |

*Reaction conditions: SO = 8.7 mmol, 600 rpm. Catalyst mol%: **CoMOF-2** = 1.8 mol%; tetrabutyl ammonium bromide (TBAB)/TBAI/KI = 2.5 mol%; $P_{CO2}$ = 1.0 bar. #Selectivity = 99%

Accordingly, **CoMOF-2** exhibits highly efficient catalytic activity with SO conversion 93% in styrene carbonate formation, under a $CO_2$ pressure of 1 bar after 8 h at 40 °C in presence of TBAB as co-catalyst (**Table 1**, entry 6). But in order to achieve 99 % SO conversion the reaction time has to increase to 12 h at 40 °C and reserved as optimized condition for further catalytic studies, retaining all other set condition (**Table 1**, entry 7). As shown in **Table 1**, barely any reaction occurs in absence of catalyst, co-catalyst or its combination at RT and 1 bar $P_{CO2}$ (**Table 1**, entry 1-3). Catalytic experiments were also performed upon increasing the temperature to 40 °C in presence of TBAB or **CoMOF-2** alone (borne only 22 and 16% SO conversion) retaining the same conditions in establishing better comparison for further experiments (**Table 1**, entry 9-11). For selection of best co-catalyst, experiments were performed using TBAB, TBAI and KI as co-catalysts. Considering the best activity, TBAB has chosen as the co-catalyst for the coupling of $CO_2$ with monosubstituted epoxides (**Table-1**, entry 4-6). Keeping $CO_2$ pressure 1 bar, SC formation using **CoMOF-2**/TBAB has been probed systematically by variation of variation of time, catalytic loading and temperature. As shown in **figure 3a**, temperature dependent catalytic activity revealed 71% SO conversion upon steady increase up to 35 ºC and almost 99% conversion was achieved at 40 ºC.

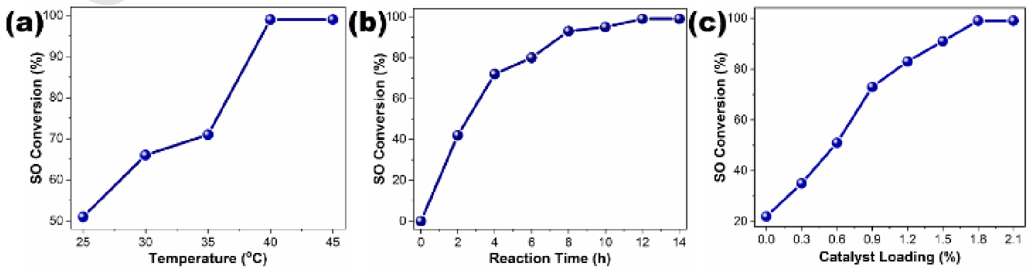

**Figure 3.** Effect of temperature (°C) (a), reaction time (b), and catalyst loading (c) on styrene carbonate formation. (Reaction conditions: SO = 8.7 mmol, Catalyst mol%: **CoMOF-2**/TBAB = 1.8/2.5 mol% (except c), $P_{CO2}$ = 1.0 bar, 40 °C (except a), 12 h except (b), 600 rpm)

Time-dependent studies in the range of 0 to 14 h exposed that SO conversion up to 80% reached within 8 h but longer duration up to 12 h has taken to achieve 99% SO conversion (**Figure 3b**). Studies of catalytic loading ranging 0-2.0 mol% exposed a gradual increment of the SO conversion reached saturation to 99% at 1.8 mol% of **CoMOF-2** (**Figure 3c**). It is noted that all catalytic experiments were performed thrice to ensure the reproducibility and the following final optimized reaction condition (SO 8.7 mmol, **CoMOF-2**/TBAB = 1.8/2.5 mol%; at 40 °C, $P_{CO2}$ 1 bar and 12 h reaction time) has been employed for further catalytic studies of different substrates.

**Table 2.** Substrate screening using **CoMOF-2** catalyst in the cycloaddition of monosubstituted epoxide with $CO_2$.*

| Entry | Substrate | Product | Yield (%) | TON[#] | TOF ($h^{-1}$) |
|---|---|---|---|---|---|
| 1 | 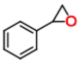 | 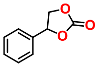 | 99 | 33 | 2.75 |
| 2 | 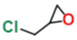 | 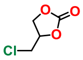 | 98 | 32 | 2.66 |
| 3 | 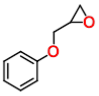 | 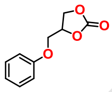 | 81 | 27 | 2.25 |
| 4 | 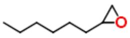 | 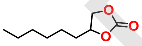 | 89 | 29 | 2.41 |
| 5 | 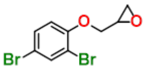 | 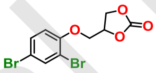 | 71 | 23 | 1.91 |
| 6 | 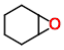 | 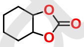 | 14 | 04 | 0.33 |

*Reaction conditions: Epoxide = 8.7 mmol, Catalyst mol%: **CoMOF-2**/TBAB = 1.8/2.5 mol%; $P_{CO2}$ = 1.0 bar, 12 h, and 40 °C, 600 rpm; [#]TON = moles of product/moles of active metal sites.

Based on optimization of **CoMOF-2** catalyst, succeeding aliphatic and aromatic substrates (styrene oxide, epichlorohydrin, 1,2-epoxy-3-phenoxypropane, 1,2-epoxyoctane and 2,4-dibromophenyl glycidyl ether) has been chosen as monosubstituted epoxides in $CO_2$ coupling reactions. The binary catalyst could convert all substrates efficiently to the corresponding cyclic carbonates under the set optimized mild reaction condition as shown in **Table 2**. Overall, the product yield for the aliphatic epoxides were good showing a decreasing trend with increase in chain length in the product formation (**Table 2**, entry 2 and 4). For aromatic epoxide, the product yield was in the range 71-99% and bulky Br substitution on the aromatic ring lowered the yield considerably may be due to the slow diffusion of retarding the substrate towards the catalytic sites by steric factor (**Table 2**, entry 1,3 and 5).

Excellent catalytic performance by **CoMOF-2**/TBAB under mild reaction condition towards monosubstituted epoxides exhilarated us to explore more challenging $CO_2$ coupling reactions with disubstituted epoxides. Catalytic cycloaddition of disubstituted epoxide with $CO_2$ is challenge and often overlooked in substrate scope due to the reaction demands development of energy efficient catalytic system. Extreme reaction conditions to support the product yield such as elevated temperature/$CO_2$ pressure and reaction time also limited the room for this scantly explored catalytic reaction. However, we have decided to explore benchmark disubstituted epoxide cyclohexene oxide (CHO) as model substrate for $CO_2$-Epoxide cycloaddition in presence of **CoMOF-2** as the catalyst.

**Table 3.** Substrate screening using **CoMOF-2** catalyst in the cycloaddition of monosubstituted epoxide with $CO_2$.*

| Entry | Catalyst/Co-catalyst | Temp. ($^o$C) | Time (h) | CHO Con. (%)$^\#$ |
|---|---|---|---|---|
| 1 | None | RT | 24 | 01 |
| 2 | **CoMOF-2** | RT | 24 | 07 |
| 3 | KI | RT | 24 | 06 |
| 4 | **CoMOF-2**/TBAB | RT | 24 | 23 |
| 5 | **CoMOF-2**/TBAI | RT | 24 | 19 |
| 6 | **CoMOF-2**/KI | RT | 24 | 42 |
| 7 | **CoMOF-2**/KI | 40 | 24 | 52 |
| 8 | **CoMOF-2**/KI | 80 | 24 | 78 |
| 9 | **CoMOF-2**/KI | 120 | 24 | 99 |
| 10 | **CoMOF-2**/KI | 120 | 12 | 86 |
| 11 | None | 120 | 24 | 06 |
| 12 | **CoMOF-2** | 120 | 24 | 14 |
| 13 | KI | 120 | 24 | 12 |

*Reaction conditions: CHO = 20 mmol, 600 rpm. Catalyst mol%: CoMOF-2 = 5 mol%; tetrabutyl ammonium bromide (TBAB)/TBAI/KI = 5 mol%; $P_{CO2}$ = 10.0 bar. #Selectivity = 99%.

Concentration of CHO substrate = 20 mmol; **CoMOF-2** = 5mol%; TBAB/TBAI/KI = 5mol% has been set and optimization experiments were performed for cyclohexene carbonate (CHC) formation as depicted in **table 3** and the details of catalytic experiment is provided in ESI. As expected, no noticeable CHO conversion was detected at RT in blank reaction, only catalyst or co-catalyst with substrate even at 10 bar $CO_2$ pressure and 24 h reaction time (**Table** 3, entry 1-3). Interestingly, the binary catalyst under the identified reaction parameters revealed encouraging results with maximum of 42% of CHO conversion expending **CoMOF-2**/KI (**Table 3**, entry 4-6). Considering the best performance of **CoMOF-2**/KI, influence of temperature on catalytic activity for cycloaddition has been investigated retaining all the other parameters intact. Thus, upon increasing the temperature to 40, 80 and 120 $^o$C retaining 10 bar $P_{CO2}$ and 24 h reaction time, CHO conversion was 52, 78 and 99% respectively (**Table 3**, entry 7-9). CHO conversion was reduced to 86% when the reaction time is restricted to 12 h at 120 $^o$C and 10 bar $P_{CO2}$ (**Table 3**, entry 10). Hence, optimized time and temperature for the reaction has been fixed 24 h and 120 $^o$C in line with maximum yield. For better comparison blank reaction, reaction with only respective catalyst and cocatalyst KI was also performed under the optimized reaction condition which showed only marginal CHO conversion (**Table 3**, entry 11-13).

To ascertain the best possible combination for optimal catalytic reaction conditions, systematic reactions for model CHO-$CO_2$ cycloaddition upon incremental variation of $CO_2$ pressure, temperature, reaction time and catalyst amounts has been investigated. Effect of pressure variation in product yield in the range 2-10 bar shown steady conversion of CHO up to 2 bar followed by an abrupt increase and 99% CHO conversion was attained at 10 bar pressure (**Figure 4a**). High solubility of $CO_2$ concentration in the liquid phase under the applied high pressure may be the reason for enhanced CHO conversion. As depicted in **figure 4b**, the efficiency of substrate conversion steadily improved upon increase in temperature and at 120 $^oC$ a maximum of 99% CHO conversion is achieved. Effect of reaction time on catalytic activity in the range of 0 to 24 h exposed increment in conversion with reaction time and 99% conversion is accomplished within 24 h (**Figure 4c**). Incremental addition of the catalyst loading experiment revealed, 99% CHO conversion is achieved at 5 mol% of **CoMOF-2** as shown in **figure 4d**. To attain maximum product yield, optimized reaction parameters such as a reaction temperature of 120 °C and $CO_2$ pressure 10 bar, 24 h reaction time with 5 mol% catalyst loading was required based on the systematic experiments conducted and retained parameters for further substrate screening catalytic experiments.

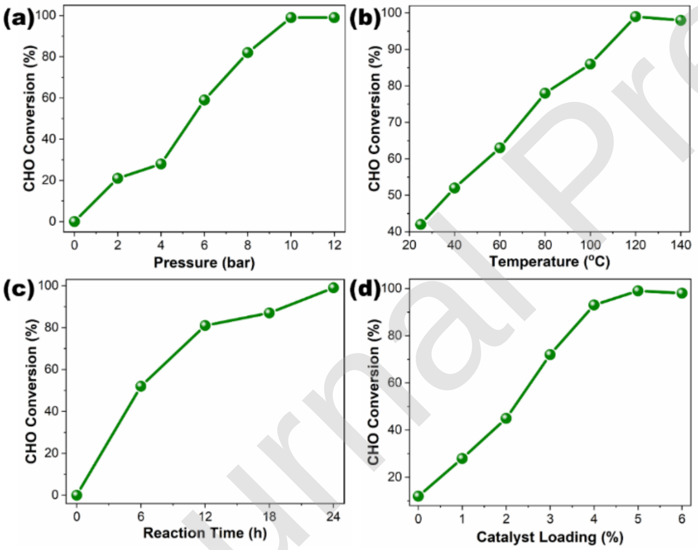

**Figure 4.** Effect of pressure (a), temperature (b), reaction time (c), and catalyst loading (d) on cyclohexene carbonate formation. (Reaction conditions: CHO = 20 mmol, Catalyst mol%: **CoMOF-2**/KI = 5/5 mol% (except d), $P_{CO2}$ = 10 bar (except a), 24 h (except c), 120 $^oC$ (except d), 600 rpm)

Disubstituted epoxides are considered difficult substrates consuming high energy input (prolonged reaction time, higher temperature/pressure) to accomplish reasonable product yield in catalytic cycloaddition reaction and scantly reported in literature. **CoMOF-2**/KI (5 mol% ) as a binary catalyst for cycloaddition reaction has been performed with various disubstituted epoxides (cyclohexene oxide, 1,2-epoxy-2-methylpropane, 2,3-epoxybutane, cyclopentene oxide, stilbene oxide and cyclooctene oxide) and $CO_2$ with the set optimized reaction conditions (10 bar, 120 °C in 24 h and 20 mmol of respective substrates). As summarized in **table 4**, all disubstituted epoxide except cyclooctene oxide sustain promising cyclic carbonate formation under the comparatively mild optimized catalytic condition. Simple disubstituted epoxides with three, five and six membered cyclic rings the product yield was in the range 89 to 99% (**Table 4**, entry1-4). Further, cyclic carbonate yield for phenyl substituted three membered epoxide was 79% and marginal yield of 9% was obtained in the case eight membered epoxide (**Table 4**, entry5-6).

**Table 4.** Substrate Screening by catalyst **CoMOF-2** in the cycloaddition of disubstituted epoxide with $CO_2$.*

| Entry | Substrate | Product | Yield (%) | TON# | TOF ($h^{-1}$) |
|---|---|---|---|---|---|
| 1 | 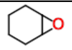 | 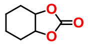 | 99 | 12 | 0.5 |
| 2 | 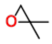 | 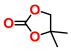 | 96 | 11 | 0.45 |
| 3 | 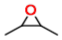 | 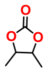 | 92 | 11 | 0.45 |
| 4 | 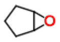 | 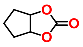 | 86 | 10 | 0.41 |
| 5 | 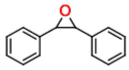 | 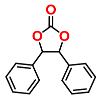 | 79 | 09 | 0.37 |
| 6 | 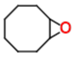 | 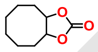 | 09 | 01 | 0.04 |

*Reaction conditions: Epoxide = 20 mmol, Catalyst mol%: **CoMOF-2**/KI = 5/5 mol%; $P_{CO2}$ = 10 bar, 24 h, and 120 °C, 600 rpm; #TON = moles of product/moles of active metal sites.

The poor catalytic efficiency and product yield, in particular for cyclooctene oxide (9%) may be probably lower reactivity of the substrate due to the bulkiness and slow diffusion in approaching the catalytically active sites. Reports on catalytic $CO_2$-disubstituted epoxide cycloaddition reactions are mainly focused on metal complex based homogeneous catalysts including metal-Schiff base complexes and organo-catalysts.[86-95] These homogenous catalysts give good yield and selectivity at harsh reaction conditions and the major concern is catalyst separation and recyclability which in turn has implication in sustainability and energy conservation. Present investigation clearly demonstrates a comprehensive study on efficacy of the MOF based heterogeneous catalyst for the conversion of disubstituted epoxides by $CO_2$ sequestration under comparatively moderate reaction condition to value added product. For better understanding and comparison, cycloaddition of $CO_2$ with styrene oxide and cyclohexene oxide with variety of catalytic material has been provided in the supporting data which also includes our recent report in this area (**Table S1-S2**). **CoMOF-2** exhibit excellent product yield and selectivity not only for monosubstituted epoxide at mild conditions but also for scarcely explored different disubstituted epoxide as an efficient heterogeneous catalytic material at moderate reaction parameters.

### *Recyclability, Proposed Catalytic Mechanism and Computational Studies*

To check the facile separation and recyclability of MOF, the catalytic products of mono and disubstituted epoxides were isolated by extraction and the catalyst was separated by centrifuge and filtration. The recovered catalyst was further purified by washing with water/methanol/acetone, dried and reused up to six repeated cycles without significant loss in catalytic activity (**Figure 5a**). PXRD/FTIR/FE-SEM data of the recycled material revealed identical pattern of the pristine compound retaining the characteristic peaks confirming the intact chemical stability and structural integrity of recycled catalyst (**Figure 5b, S2** & **S4**). To establish the transformation rate of substrates in the cycloaddition hot filtration test was performed by removing the catalyst at half the reaction time, displaying no enrichment in the product yield validating the active sites are existing in the catalyst (**Figure S30**).

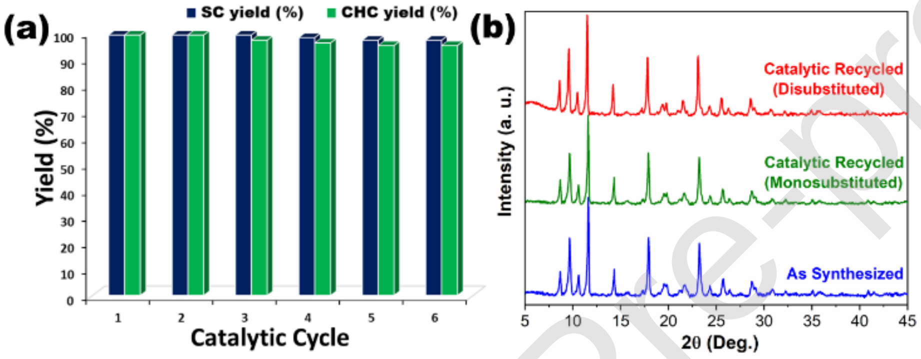

**Figure 5.** (a) Recyclability of **CoMOF-2** up to 6 catalytic cycles for styrene oxide and cyclohexene oxide conversion, (b) PXRD data of **CoMOF-2** recovered after 6 catalytic recycle for cycloaddition reaction of mono/disubstituted epoxide compared with PXRD data of as synthesized.

Plausible mechanism for **CoMOF-2**/KI catalyzed $CO_2$-cycloaddition is proposed based on literature[42,47,64,79,85,96-100] and the crystal structure of the catalyst exposing Lewis acidic metal site (by opening up weakly coordinated by the chelated carboxylate) and amide decorated Lewis basic site of **L** favoring the synergistic activation of the epoxide ring (**Figure 6a**) Presence of vacant or labile sites on the coordinated metal ions as Lewis acid and the functionalized organic ligand with Lewis basic sites in MOF can activate the epoxide moiety to enhance the catalytic activity. SXRD analysis and gas adsorption studies on **CoMOF-2** revealed low porosity and recommends the catalysis reaction probably taking place on the surface of the MOF. Presence high density Co(II) clusters with chelated labile carboxylate oxygen and the amide group on **L** can activate the epoxide ring in the cycloaddition as Lewis acidic/ basic sites. As depicted in **figure 6b** & **S8-S9**, energy profile and mechanistic pathway for $CO_2$-cycloaddition relates concurrent involvement of the Lewis Co(II) site/acyl hydrazone from **L** interacting with the epoxide oxygen facilitate ring opening. During the catalytic reaction, the activation of the epoxide ring opening is occurred by the coordination of the epoxide ring oxygen with the Co(II) Lewis site and with the pillared **L** on the catalyst surface. Simultaneously, iodide/bromide ion proceeds with nucleophilic attack on the less-hindered epoxide carbon atom. Meantime, formation of an alkyl carbonate anion takes place by interaction of $CO_2$ and negatively charged oxygen of opened epoxy ring followed by ring closure with regeneration of catalyst along with the desired catalytic product.

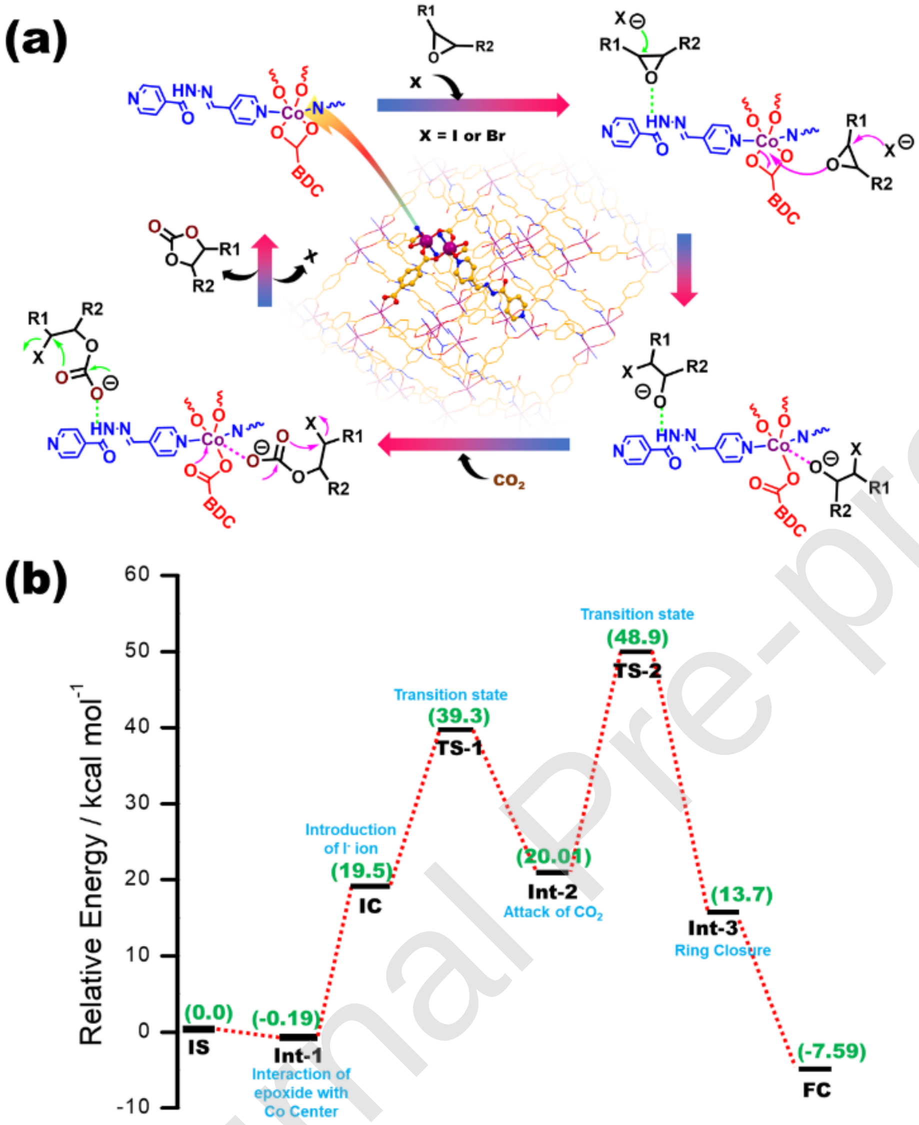

**Figure 6.** Proposed mechanism (a) and Energy profile diagram of the states calculated using DFT calculation (b) in the **CoMOF-2** catalyzed cycloaddition of epoxide and $CO_2$ to form cyclic carbonate.

The proposed mechanistic pathway is corroborated well with the DFT calculations and the experimental details for the computational studies are in the **ESI**. As shown in **figure 6b** & **S8**, the interaction of the CHO oxygen with the Cobalt (II) is initial step for the catalytic path way in the formation of intermediate (Int-1) and the energy of IS (initial structure) is close to the total energy of the cluster model of **CoMOF-2** (catalyst), nucleophile ($I^-$), $CO_2$, and CHO (isolated reactants). Upon the introduction of $I^-$ ion which was at a far off distance (>5.0 Å) from the alpha carbon ($\beta C_{(epoxide)}$) of CHO in the vicinity (Int-1), marks slight decrease in relative energy to -0.19 kcal/mol with Co(II)···O and $I^-$···alpha carbon distances 3.85 Å and

2.22 Å respectively. Subsequent ring opening and nucleophilic attack of $I^-$ on β-carbon (β$C_{(epoxide)}$) of CHO leads to an alkoxide species (IC), followed by the formation of first transition state with relative energy of 19.5 kcal/mol. During this process strong Co-$O_{(C6)}$ interaction and β$C_{(epoxide)}$-I bond formation ensued (respective inter atomic distances 2.9 Å and 2.2 Å) with the relative energy 39.3 kcal/mol for CHO ring opening (TS-1), which can be considered as the rate determining step for $CO_2$ fixation and energy difference between TS-1 and IC is 19.9 kcal/mol. The iodide ion substituted alkoxide species (TS-1) endures an intermediate state (Int-2) with a relative energy 20.01 kcal/mol followed by $CO_2$ approach at a distance 2.73Å. Oxygen anion of CHO interacts with $CO_2$ formed second transition state (TS-2) in which $CO_2$ binding takes place between the alkoxide group and Co with a relative energy 48.9 kcal/mol and in this new bond formation Co-$O_{(CO2)}$ and $O_{(CO2)}$-β$C_{(epoxide)}$ distances are 2.58 Å and 1.5 Å, respectively. The ring-closing was succeeded via new intermediate Int-3 formation with relative energy value of 13.7 kcal/mol in which the polarized carbon from $CO_2$ attacks the oxygen of CHO to form CHC (cyclohexene carbonate) through new bond $O_{(epoxide)}$-$C_{(CO2)}$. Upon CHC materialization $O_{(CO2)}$- β$C_{(epoxide)}$ is decreases from 1.5 Å to 1.4 Å whereas bon distances increases 2.9 Å from 2.6 Å and 3.58 Å from 2.4 Å for Co-$O_{(CO2)}$ and C-I bond respectively. Finally, CHC detachment along with regeneration of the catalyst is traced with an energy -7.6 kcal/mol.

## Conclusion

In summary, versatile synthetic approaches such as RT stirring for the phase pure synthesis of mixed ligand chemically stable 3D MOF (**CoMOF-2**) has been established and characterized by different analytical methods including SXRD analysis. **CoMOF-2**/TBAB or KI act as an efficient binary heterogeneous catalyst for $CO_2$ sequestration with mono/disubstituted epoxides at moderate reaction condition to value added organic carbonate with excellent yield and recyclability. $CO_2$ adsorption by **CoMOF-2**, Lewis acidic metal and the basic –NH sites in **L** enable both the interactions and activation of epoxide and $CO_2$ molecules towards excellent performance in the chemical fixation of $CO_2$. Exposed with catalytic sites involving high density of the Lewis acidic metal /basic amide across the organic ligand in **CoMOF-2**, enhances the catalytic performance by activating the epoxide ring and increasing the affinity for $CO_2$.The findings also provide insight for bulk phase pure synthesis of robust MOFs tailoring the chemical functionality towards improved catalytic performance by tuning the reaction parameters.

## Author contributions

P. Patel and B. Parmar contributed equally and performed the catalyst preparation, characterizations, catalytic application, data analysis and write up. Dr. R. S. Pillai carried out computational calculations, related write up and offered helpful suggestions. A. Ansari performed the catalytic tests and analysis. Dr. E. Suresh and Dr. N. H. Khan conceived the idea, supervise overall direction/planning of the project and write up.

## Conflicts of interest

There are no conflicts to declare.

## Acknowledgments

The registration number of this publication is CSIR-CSMCRI – 107/2019. Financial support from CSIR-SRF (BP), DST Project HCP0009 (PP) and analytical support by AESD&CIF of CSIR-CSMCRI is gratefully acknowledged. We thank Ms. Mohali Acharya for PXRD, Dr. Vinod Boricha for NMR data, Mr. Jayesh Chaudhari for FE-SEM analysis, Mr. Vinod Kumar Agrawal for FTIR data, Mr. Satyaveer Gothwal for TGA data, Mr. Viral Vakani for CHN analysis and Mr. Harpalsinh Rathod for $N_2$/$CO_2$-adsorption desorption analysis. R.S.P. gratefully acknowledges the Science and Engineering Research Board (SERB), Department of Science and Technology (DST), Govt. of India, for the financial support by the award of Start-up Research Grant (SERB-SRG) with reference SRG/2019/000912. R.S.P. thank High Performance Computing Center, SRM Institute of Science and Technology for providing the computational facility.

## References

[1] P.N. Pearson, M.R. Palmer, Nature 406 (2000) 695-699.
[2] T. Sakakura, J.-C. Choi, H. Yasuda, Chem. Rev. 107 (2007) 2365-2387.

[3] I. Omae, Coord. Chem. Rev. 256 (2012) 1384-1405.

[4] M.E. Boot-Handford, J.C. Abanades, E.J. Anthony, M.J. Blunt, S. Brandani, N. Mac Dowell, J.R. Fernández, M.-C. Ferrari, R. Gross, J.P. Hallett, R.S. Haszeldine, P. Heptonstall, A. Lyngfelt, Z. Makuch, E. Mangano, R.T.J. Porter, M. Pourkashanian, G.T. Rochelle, N. Shah, J.G. Yao, P.S. Fennell, Energy Environ. Sci. 7 (2014) 130-189.

[5] F.A. Rahman, M.M.A. Aziz, R. Saidur, W.A.W.A. Bakar, M. Hainin, R. Putrajaya, N.A. Hassan, Renew. Sust. Ene. Rev. 71 (2017) 112-126.

[6] J. Artz, T.E. Müller, K. Thenert, J. Kleinekorte, R. Meys, A. Sternberg, A. Bardow, W. Leitner, Chem. Rev. 118 (2018) 434-504.

[7] B. Chen, L. Wang, S. Gao, ACS Catal. 5 (2015) 5851-5876.

[8] M.T. Schümperli, C. Hammond, I. Hermans, ACS Catal. 2 (2012) 1108-1117.

[9] J. Han, V.A. Soloshonok, K.D. Klika, Z. Drabowicz, A. Wzorek, Chem. Soc. Rev. 47 (2018) 1307-1350.

[10] K. Sordakis, C. Tang, L.K. Vogt, H. Junge, P.J. Dyson, M. Beller, G. Laurenczy, Chem. Rev. 118 (2018) 372-433.

[11] D.J. Darensbourg, M.W. Holtcamp, Coord. Chem. Rev. 153 (1996) 155-174.

[12] C. Martín, G. Fiorani, A.W. Kleij, ACS Catal. 5 (2015) 1353-1370.

[13] C. Copÿret, M. Chabanas, R.P. Saint-Arroman, J. M. Basset, Angew. Chem. Int. Ed. 42 (2003) 156-181.

[14] J.A. Widegren, R.G. Finke, J. Mol. Catal. A: Chem. 198 (2003) 317-341.

[15] J.-Q. Wang, D.-L. Kong, J.-Y. Chen, F. Cai, L.-N. He, J. Mol. Catal. A: Chem. 249 (2006) 143-148.

[16] M. North, R. Pasquale, C. Young, Green Chem. 12 (2010) 1514-1539.

[17] M. Cokoja, M.E. Wilhelm, M.H. Anthofer, W.A. Herrmann, F.E. Kühn, ChemSusChem 8 (2015) 2436-2454.

[18] R.K. Tak, P. Patel, S. Subramanian, R.I. Kureshy, N.H. Khan, ACS Sustainable Chem. Eng. 6 (2018) 11200-11205.

[19] S. Subramanian, J. Park, J. Byun, Y. Jung, C.T. Yavuz, ACS Appl. Mater. Interfaces, 10 (2018) 9478-9484.

[20] J.H. Clements, Reactive Applications of Cyclic Alkylene Carbonates, Ind. Eng. Chem. Res. 42 (2003) 663-674.

[21] G.W. Coates, D.R. Moore, Angew. Chem. Int. Ed. 43 (2004) 6618-6639.

[22] D.J. Darensbourg, Chem. Rev. 107 (2007) 2388-2410.

[23] B. Schäffner, F. Schäffner, S. P. Verevkin, A. Börner, Chem. Rev. 110 (2010) 4554-4581.

[24] C. Beattie, M. North, P. Villuendas, Molecules 16 (2011) 3420-3432.

[25] S.H. Kim, S.H. Hong, ACS Catal. 4 (2014) 3630-3636.

[26] J. Yun, L. Zhang, Q. Qu, H. Liu, X. Zhang, M. Shen, H. Zheng, Electrochim. Acta 167 (2015) 151-159.

[27] A. Kumar, T. Janes, N.A. Espinosa-Jalapa, D. Milstein, Angew. Chem. Int. Ed. 57 (2018) 12076-12080.

[28] H.-C. Zhou, J.R. Long, O.M. Yaghi, Chem. Rev. 112 (2012) 673-674.

[29] A. Kirchon, L. Feng, H.F. Drake, E.A. Joseph, H.-C. Zhou, Chem. Soc. Rev. 47 (2018) 8611-8638.

[30] W.P. Lustig, S. Mukherjee, N.D. Rudd, A.V. Desai, J. Li, S.K. Ghosh, Chem. Soc. Rev. 46 (2017) 3242-3285.

[31] H. Wang, Q.-L. Zhu, R. Zou, Q. Xu, Chem 2 (2017) 52-80.

[32] P. Horcajada, R. Gref, T. Baati, P.K. Allan, G. Maurin, P. Couvreur, G. Férey, R.E. Morris, C. Serre, Chem. Rev. 112 (2012) 1232-1268.

[33] J. Liu, C. Wöll, Chem. Soc. Rev. 46 (2017) 5730-5770.

[34] J.Y. Lee, O.K. Farha, J. Roberts, K.A. Scheidt, S.T. Nguyen, J.T. Hupp, Chem. Soc. Rev. 38 (2009) 1450-1459.

[35] M. Yoon, R. Srirambalaji, K. Kim, Chem. Rev. 112 (2012) 1196-1231.

[36] J. Liu, L. Chen, H. Cui, J. Zhang, L. Zhang, C.-Y. Su, Chem. Soc. Rev. 43 (2014) 6011-6061.

[37] L. Zhu, X.-Q. Liu, H.-L. Jiang, L.-B. Sun, Chem. Rev. 117 (2017) 8129-8176.

[38] A.C. Kathalikkattil, R. Babu, J. Tharun, R. Roshan, D.-W. Park, Catal. Surv. Asia 19 (2015) 223-235.

[39] J.W. Maina, C. Pozo-Gonzalo, L. Kong, J. Schütz, M. Hill, L.F. Dumée, Mater. Horiz. 4 (2017) 345-361.

[40] C.A. Trickett, A. Helal, B.A. Al-Maythalony, Z.H. Yamani, K.E. Cordova, O.M. Yaghi, Nat. Rev. Mater. 2 (2017) 17045.

[41] H. He, J.A. Perman, G. Zhu, S. Ma, small 12 (2016) 6309-6324.

[42] M. Ding, R.W. Flaig, H.-L. Jiang, O.M. Yaghi, Chem. Soc. Rev. 48 (2019) 2783-2828.

[43] M. Zhu, D. Srinivas, S. Bhogeswararao, P. Ratnasamy, M.A. Carreon, Catal. Commun. 32 (2013) 36-40.

[44] V. Guillerm, Ł.J. Weseliński, Y. Belmabkhout, A.J. Cairns, V. D'Elia, Ł. Wojtas, K. Adil, M. Eddaoudi, Nat. Chem. 6 (2014) 673-680.

[45] W.-Y. Gao, L. Wojtas, S. Ma, Chem. Commun. 50 (2014) 5316-5318.

[46] P. -Z. Li, X.-J. Wang, J. Liu, J.S. Lim, R.-Q. Zou, Y.-L. Zhao, J. Am. Chem. Soc. 138 (2016) 2142-2145.

[47] W.-Y. Gao, Y. Chen, Y.-H. Niu, K. Williams, L. Cash, P.J. Perez, L. Wojtas, J.-F. Cai, Y.-S. Chen, S. Ma, Angew. Chem. Int. Ed. 53 (2014) 2615-2619.

[48] E.E. Macias, P. Ratnasamy, M.A. Carreon, Catal. Today 198 (2012) 215-218.

[49] D. Feng, W.-C. Chung, Z. Wei, Z.-Y. Gu, H.-L. Jiang, Y.-P. Chen, D.J. Darensbourg, H.-C. Zhou, J. Am. Chem. Soc. 135 (2013) 17105-17110.

[50] M.H. Beyzavi, R.C. Klet, S. Tussupbayev, J. Borycz, N.A. Vermeulen, C.J. Cramer, J.F. Stoddart, J.T. Hupp, O.K. Farha, J. Am. Chem. Soc. 136 (2014) 15861-15864.

[51] A.C. Kathalikkattil, R. Babu, R.K. Roshan, H. Lee, H. Kim, J. Tharun, E. Suresh, D.-W. Park, J. Mater. Chem. A 3 (2015) 22636-22647.

[52] W.-Y. Gao, C.-Y. Tsai, L. Wojtas, T. Thiounn, C.-C. Lin, S. Ma, Inorg. Chem. 55 (2016) 7291-7294.

[53] Y.-H. Han, Z.-Y. Zhou, C.-B. Tian, S.-W. Du, Green Chem. 18 (2016) 4086-4091.

[54] H. Xu, B. Zhai, C.-S. Cao, B. Zhao, Inorg. Chem. 55 (2016) 9671-9676.

[55] M.H. Alkordi, L.J. Weseliński, V. D'Elia, S. Barman, A. Cadiau, M.N. Hedhili, A.J. Cairns, R.G. AbdulHalim, J.-M. Basset, M. Eddaoudi, J. Mater. Chem. A 4 (2016) 7453-7460.

[56] R. Babu, A.C. Kathalikkattil, R. Roshan, J. Tharun, D.-W. Kim, D.-W. Park, Green Chem. 18 (2016) 232-242.

[57] M. Taherimehr, B. Van de Voorde, L.H. Wee, J.A. Martens, D.E. De Vos, P.P. Pescarmona, ChemSusChem 10 (2017) 1283-1291.

[58] W.-Z. Qiao, H. Xu, P. Cheng, B. Zhao, Cryst. Growth Des. 17 (2017) 3128-3133.

[59] M. Ding, S. Chen, X.-Q. Liu, L.-B. Sun, J. Lu, H.-L. Jiang, ChemSusChem 10 (2017) 1898-1903.

[60] V. Sharma, D. De, R. Saha, R. Das, P.K. Chattaraj, P.K. Bharadwaj, Chem. Commun. 53 (2017) 13371-13374.

[61] P.T.K. Nguyen, H.T.D. Nguyen, H.N. Nguyen, C.A. Trickett, Q.T. Ton, E. Gutiérrez-Puebla, M.A. Monge, K.E. Cordova, F. Gándara, ACS Appl. Mater. Interfaces 10 (2018) 733-744.

[62] J. Zhu, P.M. Usov, W. Xu, P.J. Celis-Salazar, S. Lin, M.C. Kessinger, C. Landaverde-Alvarado, M. Cai, A.M. May, C. Slebodnick, D. Zhu, S.D. Senanayake, A.J. Morris, J. Am. Chem. Soc. 140 (2018) 993-1003.

[63] X.-Y. Li, L.-N. Ma, Y. Liu, L. Hou, Y.-Y. Wang, Z. Zhu, ACS Appl. Mater. Interfaces 10 (2018) 10965-10973.

[64] H. He, Q. Sun, W. Gao, J.A. Perman, F. Sun, G. Zhu, B. Aguila, K. Forrest, B. Space, S. Ma, Angew. Chem. Int. Ed. 57 (2018) 4657-4662.

[65] W. Meng, Y. Zeng, Z. Liang, W. Guo, C. Zhi, Y. Wu, R. Zhong, C. Qu, R. Zou, ChemSusChem 11 (2018) 3751-3757.

[66] C.-S. Cao, Y. Shi, H. Xu, B. Zhao, Dalton Trans. 47 (2018) 4545-4553.

[67] K. Epp, A.L. Semrau, M. Cokoja, R.A. Fischer, ChemCatChem 10 (2018) 3506-3512.

[68] S.N. Ansari, P. Kumar, A.K. Gupta, P. Mathur, S.M. Mobin, Inorg. Chem. 58 (2019) 9723-9732.

[69] N. Sharma, S.S. Dhankhar, C.M. Nagaraja, Microporous Mesoporous Mater. 280 (2019) 372-378.

[70] M. Singh, P. Solanki, P. Patel, A. Mondal, S. Neogi, Inorg. Chem. 58 (2019) 8100-8110.

[71] J.F. Kurisingal, Y. Rachuri, R.S. Pillai, Y. Gu, Y. Choe, D.-W. Park, ChemSusChem 12 (2019) 1033-1042.

[72] B. Ugale, S. Kumar, T.J. Dhilip Kumar, C.M. Nagaraja, Inorg. Chem. 58 (2019) 3925-3936.

[73] M. Bahadori, S. Tangestaninejad, M. Bertmer, M. Moghadam, V. Mirkhani, I. Mohammadpoor-Baltork, R. Kardanpour, F. Zadehahmadi, ACS Sustainable Chem. Eng. 7 (2019) 3962-3973.

[74] J.F. Kurisingal, Y. Rachuri, Y. Gu, Y. Choe, D.-W. Park, Chem. Eng. J. (2019) DOI: 10.1016/j.cej.2019.05.061.

[75] G. Jin, D. Sensharma, N. Zhu, S. Vaesen, W.A. Schmitt, Dalton Trans. 48 (2019) 15487-15492.

[76] P. Patel, B. Parmar, R.I. Kureshy, N.H. Khan, E. Suresh, ChemCatChem 10 (2018) 2401-2408.

[77] P. Patel, B. Parmar, R.I. Kureshy, N.H. Khan, E. Suresh, Dalton Trans. 47 (2018) 8041-8051.

[78] B. Parmar, P. Patel, R.I. Kureshy, N.H. Khan, E. Suresh, Chem. Eur. J. 24 (2018) 15831-15839.

[79] B. Parmar, P. Patel, R.S. Pillai, R.I. Kureshy, N.H. Khan, E. Suresh, J. Mater. Chem. A 7 (2019) 2884-2894.

[80] J. An, S.J. Geib, N.L. Rosi, J. Am. Chem. Soc. 132 (2010) 38-39.

[81] B. Zheng, J. Bai, J. Duan, L. Wojtas, M.J. Zaworotko, J. Am. Chem. Soc. 133 (2011) 748-751.

[82] K. Roztocki, D. Jędrzejowski, M. Hodorowicz, I. Senkovska, S. Kaskel, D. Matoga, Inorg. Chem. 55 (2016) 9663-9670.

[83] R.W. Flaig, T.M. Osborn Popp, A.M. Fracaroli, E.A. Kapustin, M.J. Kalmutzki, R.M. Altamimi, F. Fathieh, J.A. Reimer, O.M. Yaghi, J. Am. Chem. Soc. 139 (2017) 12125-12128.

[84] M. Chen, S. Chen, W. Chen, B.E.G. Lucier, Y. Zhang, A. Zheng, Y. Huang, Chem. Mater. 30 (2018) 3613-3617.

[85] B. Parmar, P. Patel, R.S. Pillai, R.K. Tak, R.I. Kureshy, N.H. Khan, E. Suresh, Inorg. Chem. 58 (2019) 10084-10096.

[86] T. Werner, N. Tenhumberg, H. Büttner, ChemCatChem 6 (2014) 3493-3500.

[87] C. Miceli, J. Rintjema, E. Martin, E.C. Escudero-Adán, C. Zonta, G. Licini, A.W. Kleij, ACS Catal. 7 (2017) 2367-2373.

[88] S. Sopeña, E. Martin, E.C. Escudero-Adán, A.W. Kleij, ACS Catal. 7 (2017) 3532-3539.

[89] F. Chen, N. Liu, B. Dai, ACS Sustainable Chem. Eng. 5 (2017) 9065-9075.

[90] J. Steinbauer, T. Werner, ChemSusChem 10 (2017) 3025-3029.

[91] T. Jose, S. Cañellas, M.A. Pericàs, A.W. Kleij, Green Chem. 19 (2017) 5488-5493.

[92] F. Chen, D. Chen, L. Shi, N. Liu, B. Dai, J. $CO_2$ Util. 16 (2016) 391-398.

[93] F. de la Cruz-Martínez, J. Martínez, M.A. Gaona, J. Fernández-Baeza, L.F. Sánchez-Barba, A.M. Rodríguez, J.A. Castro-Osma, A. Otero, A. Lara-Sánchez, ACS Sustainable Chem. Eng. 6 (2018) 5322-5332.

[94] C. Maeda, J. Shimonishi, R. Miyazaki, J. Hasegawa, T. Ema, Chem. Eur. J. 22 (2016) 6556-6563.

[95] Y. Wang, Y. Qin, X. Wang, F. Wang, Catal. Sci. Technol. 4 (2014) 3964-3972.

[96] J. Kim, S.-N. Kim, H.-G. Jang, G. Seo, W.-S. Ahn, Appl. Catal. A: Gen. 453 (2013) 175-180.

[97] X. Guo, Z. Zhou, C. Chen, J. Bai, C. He, C. Duan, ACS Appl. Mater. Interfaces 8 (2016) 31746-31756.

[98] R. Babu, R. Roshan, A.C. Kathalikkattil, D.W. Kim, D.-W. Park, ACS Appl. Mater. Interfaces 8 (2016) 33723-33731.

[99] B.-B. Lu, J. Yang, Y.-Y. Liu, J.-F. Ma, Inorg. Chem. 56 (2017) 11710-11720.

[100] P.-Z. Li, X.-J. Wang, J. Liu, H.S. Phang, Y. Li, Y. Zhao, Chem. Mater. 29 (2017) 9256-9261.